UCRL-JRNL-223505

Self-Consistent Simulations of Heavy-Ion Beams Interacting with Electron-Clouds

J.-L. Vay, M. A. Furman, P. A. Seidl, R. H. Cohen, A. Friedman, D. P. Grote, M. Kireeff Covo, A. W. Molvik, P. H. Stoltz, S. Veitzer, J. P. Verboncoeur

August 8, 2006

Disclaimer

Self-consistent simulations of heavy-ion beams interacting with electron-clouds.

J.-L. Vay,[1,*] M. A. Furman,[1] P. A. Seidl,[1] R. H. Cohen,[2] A. Friedman,[2] D. P. Grote,[2]
M. Kireeff Covo,[2] A. W. Molvik,[2] P. H. Stoltz,[3] S. Veitzer,[3] and J. P. Verboncoeur[4]

[1]LBNL, CA, USA
[2]LLNL, CA, USA
[3]Tech-X Corporation, USA
[4]UC Berkeley, USA
(Dated: July 19, 2006)

Electron-clouds and rising desorbed gas pressure limit the performance of many existing accelerators and, potentially, that of future accelerators including heavy-ion warm-dense matter and fusion drivers. For the latter, self-consistent simulation of the interaction of the heavy-ion beam(s) with the electron-cloud is necessary. To this end, we have merged the two codes WARP (HIF accelerator code) and POSINST (high-energy e-cloud build-up code), and added modules for neutral gas molecule generation, gas ionization, and electron tracking algorithms in magnetic fields with large time steps. The new tool is being benchmarked against the High-Current Experiment (HCX) and good agreement has been achieved. The simulations have also aided diagnostic interpretation and have identified unanticipated physical processes. We present the "roadmap" describing the different modules and their interconnections, along with detailed comparisons with HCX experimental results, as well as a preliminary application to the modeling of electron clouds in the Large Hadron Collider.

I. INTRODUCTION

The steadily increasing beam intensity required in operational and upcoming accelerators leads to growing concerns over the degradation of beam emittance due to electron cloud effect and gas pressure rise [1], and is of particular importance for the high-intensity accelerators envisioned for Heavy Ion Inertial Fusion (HIF) drivers and Warm-Dense Matter (WDM) studies. Accurate prediction necessitates a detailed understanding of the physical processes at play with a quantification of the relative importance of various effects. To this end, we have undertaken the development of a new generation of computer simulation code in conjunction with detailed measurements from a small but heavily diagnosed dedicated experiment, for extensive

*jlvay@lbl.gov

benchmarking and code validation. We provide here a brief overview of the simulation code and the dedicated experiment, and present recent results, focusing on the dynamics of electrons in the magnetic quadrupole section of the High-Current Experiment (HCX) [2], and a preliminary application to the modeling of electron clouds in the Large Hadron Collider (LHC) [3].

II. THE WARP/POSINST SIMULATION PACKAGE

The simulation tool is based on a merge of the Heavy Ion Fusion accelerator code WARP [4] and the High-Energy Physics electron cloud code POSINST [5, 6], supplemented by additional modules for gas generation and ionization [7], as well as ion-induced electron emission from the Tech-X package TxPhysics [8]. The package allows for multi-dimensional (2-D or 3-D) modeling of a beam in an accelerator lattice and its interac-

tion with electron clouds generated from photon-induced, ion-induced or electron-induced emission at walls, or from ionization of background and desorbed gas. The generation and tracking of all species (beams particles, ions, electrons, gas molecules) is performed in a self-consistent manner (the electron, ion and gas distributions can also be prescribed -if needed- for special study or convenience). The code runs in parallel and benefits from adaptive mesh refinement [9], particles sub-cycling [10] and a new "drift-Lorentz" particle mover for tracking charged particles in magnetic fields using large time steps [11, 12]. These advanced numerical techniques allow for significant speed-up in computing time (orders of magnitude) relative to brute-force integration techniques, allowing for self-consistent simulations of electron-cloud effects and beam dynamics, which were out of reach with previously available tools.

A. The "roadmap"

We have established a list of different functional modules, and their inter-relationships, that are ultimately needed to reach self-consistency for the modeling of HIF beams with e-cloud and gas, and have summarized it in a block diagram (see Fig. 1). We can imagine this as a "roadmap" of a self-consistent modeling capability of electron clouds effects. The central block of the roadmap is a self-consistent PIC module that follows the beam through an accelerator lattice with its self-field and images at the wall. Ions from the beam halo that strike the wall can desorb neutrals and electrons that have enough time to reach the beam before the end of the pulse, and interact with it. The time-dependent motion of neutrals and electrons must therefore be tracked. The gas can be ionized by beam ions and electrons, leading to new electrons and ions that must be tracked as well. All these particles can hit the walls and produce more neutrals and electrons. Finally, beam ions can be reflected at the wall, and charge-exchange reactions can occur in the gas. More details on the anaysis that led to the establishment of this roadmap can be found in [11–13, 15].

B. New features

We briefly describe here the features added to the WARP-POSINST capabilities. More detailed descriptions can be found in [7, 11].

1. New interpolated mover

Self-consistent simulation of electrons and ions requires simulation of electrons in the quadrupole magnets as well as in the gaps between magnets, and running the simulation long enough to simulate the passage of the ion beam. This results in a broad range of time scales, ranging from the electron cyclotron period ($10^{-11} - 10^{-10}$ s) through the ion beam transit time ($10^{-7} - 10^{-5}$ s) through a fringe field or a series of lattice elements. The shortest electron cyclotron period is typically one to two orders of magnitude smaller than the next-smallest timescale, usually the electron bounce time in the combined beam-potential and magnetic wells. To deal with this large range of time scales in a unified manner, we have developed a mover for electrons that interpolates between full electron dynamics and drift kinetics (for more details, see [11]).

2. Gas module

Impact of energetic ions with surfaces can lead to desorption of neutral atoms or molecules. At high beam energies, characteristic of the HIF and HEP applications, electronic sputtering is the dominant mechanism. In this mechanism, the incident energetic ion transfers kinetic energy to the electrons in the vacuum chamber material, transporting, in turn, the energy to the surface and to the impurities adsorbed in the lattice. The desorption yield depends on energy and angle of impact, as well as material properties and surface history. Because the dependence of the yield is difficult to characterize for technical surfaces, in the model the yield at normal incidence is specified by a phenomenological quantity. The angular dependence of the yield is then characterized by the impact angle, conventionally measured from the surface normal. The enhancement of
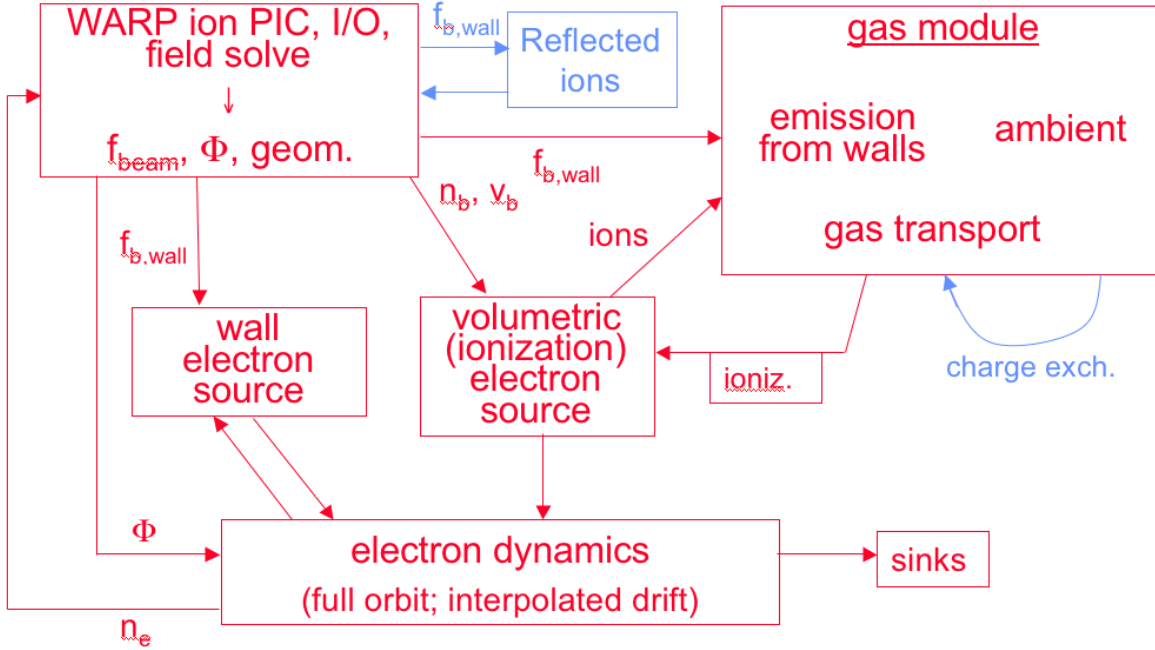
FIG. 1: "Roadmap" describing the different functional modules, and their inter-relationships, that are ultimately needed to reach self-consistency for the modeling of HIF beams with e-cloud and gas. At the time of this writing, most modules are operational, excepting the "reflected ions" and the "charge exchange" modules that are still being developed.

the yield at large angle (near grazing incidence) is possibly due to the enhanced backscatter of ions, as calculated by Molvik [13] using the SRIM code [14]. These backscattered ions result in an increase over the normal yield Y_0 by nearly a factor of 2 near grazing incidence,

$$\frac{Y(\theta)}{Y_0} = 1 + 1.82 \times 10^{-4} \exp(5.16\theta), \quad (1)$$

where θ is the angle of incidence measured in radians.

The model for the energy and angular distribution of the desorbed neutrals is based on molecular dynamics calculations (for more details, see [7]).

3. Ionization module

The background gas, or the gas generated by wall desoption from beam ion impact, can be ionized (eventually fragmented) by the beam ions, gas ions or electrons. Conversely, the interaction between the gas and the beam can lead to stripping, or capture, of electrons by the beam ions. We track these events using a Monte Carlo scheme similar to the one described in [16], where, for simplicity, we make the additional assumption (valid for current applications) that the gas reservoir is large enough, and the cross-sections are small enough, that the depletion of gas due to its ionization can be neglected (for more details, see [7]).

III. THE HIGH CURRENT EXPERIMENT

The High Current Experiment [2], located at Lawrence Berkeley National Laboratory, consists of an injector producing a singly-charged Potassium ion beam (K+) at 1 MeV kinetic energy, followed by a transport lattice made of a matching section, a ten-quadrupole electrostatic section and a four-quadrupole magnetic section. The flat top of the beam pulse reaches 180 mA and its duration is 4 μs (see Fig. 2).

FIG. 3: HCX in region of 4 quadrupole magnets, with clearing electrode rings between magnets and a suppressor electrode ring after the last magnet.

IV. RECENT STUDY OF DYNAMICS OF ELECTRONS IN A MAGNETIC QUADRUPOLE

For convenience, we label the electrons created by the beam hitting the end wall as "primary", while we label the electrons created by the primary electrons hitting the vacuum pipe surrounding the magnets as "secondary" (these encompass any subsequent generation of electrons). The primary electrons created at the end plate and propagating upstream can enter only two quadrants of the fourth (last) magnet, because of the sign of the $\mathbf{E} \times \mathbf{B}$ drift, and then drift upstream. The current measured by clearing electrode (c) is compared with simulation in Fig. 4, in the case where the suppressor ring electrode was left grounded to allow electrons to propagate upstream, and the three clearing electrodes were biased to +9 kV. The simulation and experimental results agree on the magnitude and frequency ($\sim$ 10 MHz) of the observed oscillations.
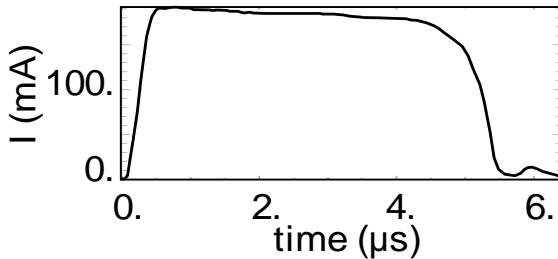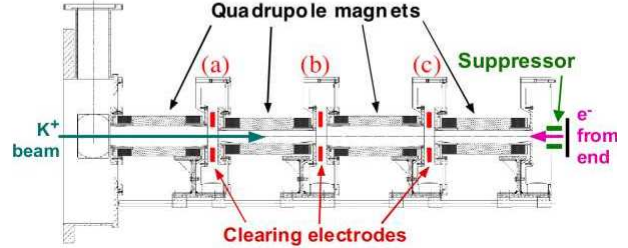

FIG. 2: Beam current history recorded from Faraday cup measurement at the exit of the electrostatic section (entrance of the magnetic section).

We study electron effects in the magnetic section [13, 17], shown in Fig. 3. A suppressor ring electrode, surrounding the beam after it exits the last quadrupole magnet, can be biased to −10 kV to prevent ion-induced electron emission off an end wall (a slit plate) from reaching the magnets, or can be left unbiased to allow electrons emitted from the end wall to freely flow upstream into the magnets. There is also a series of three clearing electrodes, labeled (a), (b) and (c) in Fig. 3, in the drift regions between quadrupole magnets, which can be biased positively to draw off electrons from between any pair of magnets. The current that flows in and out of these clearing electrodes is monitored in the experiment and is compared to simulation results for benchmarking.

Simulation results reveal that these time-dependent oscillations recorded by clearing electrode (c) are related to bunching of electrons drifting upstream in the fourth magnet. The effect of this bunching is revealed in the plot of line charge densities in Fig. 5 where oscillations of large amplitude and wavelength of approximately 5 cm are observed in the electron density in the fourth magnetic quadrupole. The effect is so pronounced that at the peak the electron line charge density reaches 1.5 times the beam line charge density. The bunching of electrons itself is re-

vealed in Fig. 6 where electrons bunches are easily observable from the middle of the quadrupole and upstream. The over-neutralization of the beam space-charge by these electron bunches is evident in Fig. 7 where islands of negative potential are formed at the location of the bunches. Although some possible candidate explanations have been eliminated (electron-ion two-stream instability for example) the nature of these oscillations has not yet been firmly identified and other possibilities, such as the Kelvin-Helmholtz instability, are under active investigation.
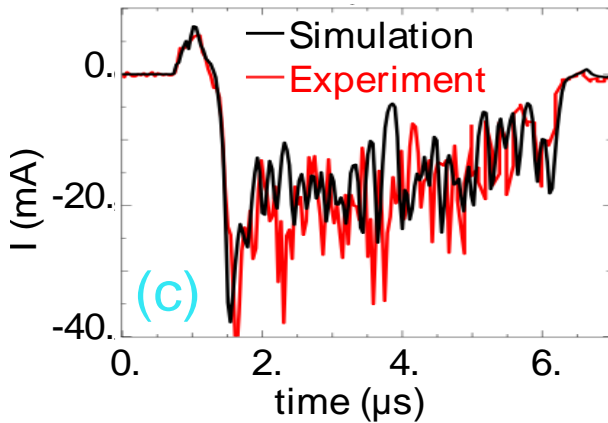

FIG. 4: Current history at clearing electrodes (c): red - recorded on HCX experiment, black - WARP-POSINST simulation of HCX.
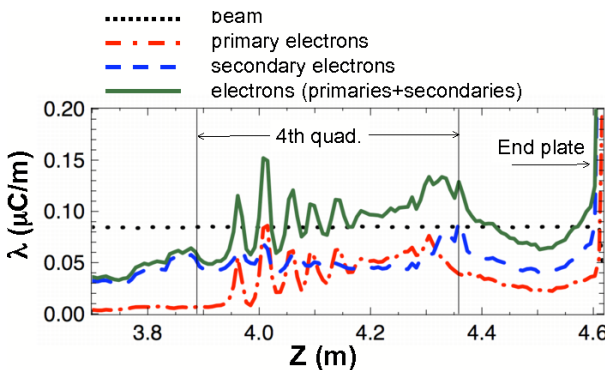

FIG. 5: Line charge density λ (absolute value), from WARP-POSINST simulation of HCX at $t = 3$ μs.

V. APPLICATION TO HIGH-ENERGY PHYSICS ACCELERATORS

We have also applied the WARP-POSINST code to the modeling of a train of bunches in one LHC FODO cell. The magnetic fields in the FODO cell used in our simulation have nominal values for 7 TeV beam energy, with geometry, dimensions and optics as specified in the LHC CDR [3]. However, for the purposes of these preliminary studies, we have used the following simplifications: (1) all cell magnets other than dipoles and quadrupoles are not included (actually, replaced by drifts); and (2) magnetic edge fields are neglected. As for the bunch train, we represent it by a succession of identical bunches with nominal intensity and emittances, and appropriate phase shifts, but we use the following simplifications: (3) periodic boundary conditions in the longitudinal dimension, both for the beam and for the electrons (so that, effectively, the model represents a circular "storage ring" consisting of a single FODO cell); and (4) the energy spread is zero (all particles have nominal energy).

We consider here only one source of primary electrons, namely the photoelectric effect from synchrotron radiation striking the walls of the chamber because, at top energy, this mechanism is by far the dominant one. We assume that the effective quantum efficiency is 0.1, so that 1.27×10^{-3} photoelectrons are generated on the chamber surface per proton per meter of beam traversal, and that the effective photon reflectivity is 20% (i.e., 80% of the photoelectrons are generated on the illuminated part of the beam screen, while 20% are generated uniformly around the perimeter of the beam screen cross-section). Finally, as an initial example for illustration purposes, we set the peak value of the secondary emission yield to 2.0 [6]. A snapshot from the simulation of a train of five bunches is shown in Fig. 8, showing the five bunches propagating in one LHC FODO cell, interacting with electrons from photo-emission and secondary emission.

While it will be a valuable tool to study in detail the beam and electron clouds for many turns, the 3-D self-consistent approach, even with the mesh refinement, sub-cycling and advanced particle pusher capabilities, must be supplemented
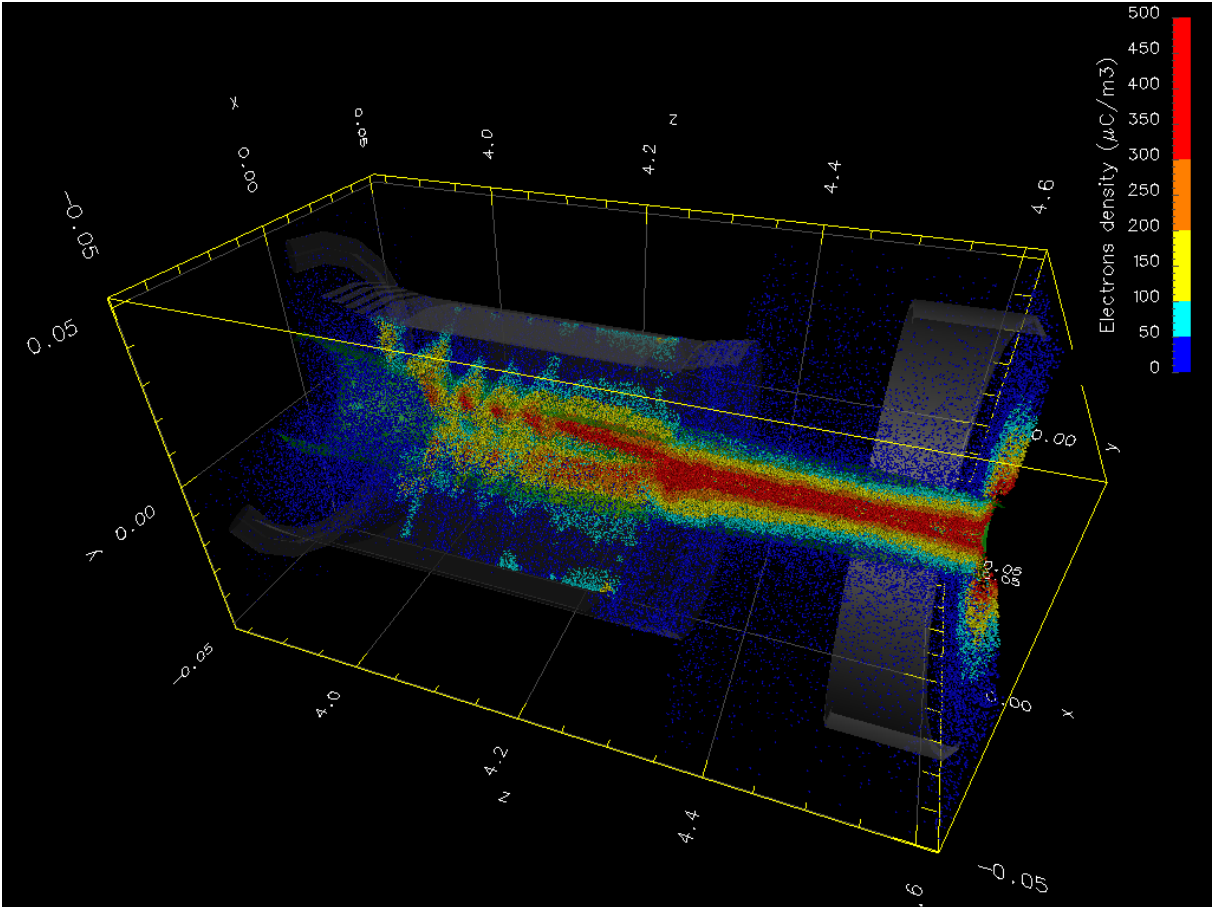
FIG. 6: Snapshot of electron macroparticles, colored according to charge density (absolute value), from WARP-POSINST simulation of HCX at $t = 3$ μs.

by a simplified description, in order to allow parametric studies of the thousands of turns (or more) that are required for the modeling of slow emittance growth [19], which is a growing concern for LHC. Thus we will implement a mode of operation similar to the ones in the codes HEAD-TAIL [20] or QUICKPIC [21], for example, where the beam is followed in three dimensions while the electrons are represented as two-dimensional slices passing through the beam. We will also explore the possible existence, and potentialities, of intermediate modes of operations, with a level of description somewhere in between this reduced mode and the full three-dimensional self-consistent mode.

VI. CONCLUSION

We have developed a three-dimensional self-consistent code suite which includes advanced numerical methods, allowing the modeling of configurations which were out of reach with previously available tools. Benchmarking against the HCX experiment has provided some very good qualitative and quantitative agreements, and is being pursued actively in order to fully validate the code and the embodied physical model. The modeling tool is also being applied to the self-consistent modeling of electron cloud effects in the Large Hadron Collider (CERN), the largest accelerator for High-Energy Physics re-
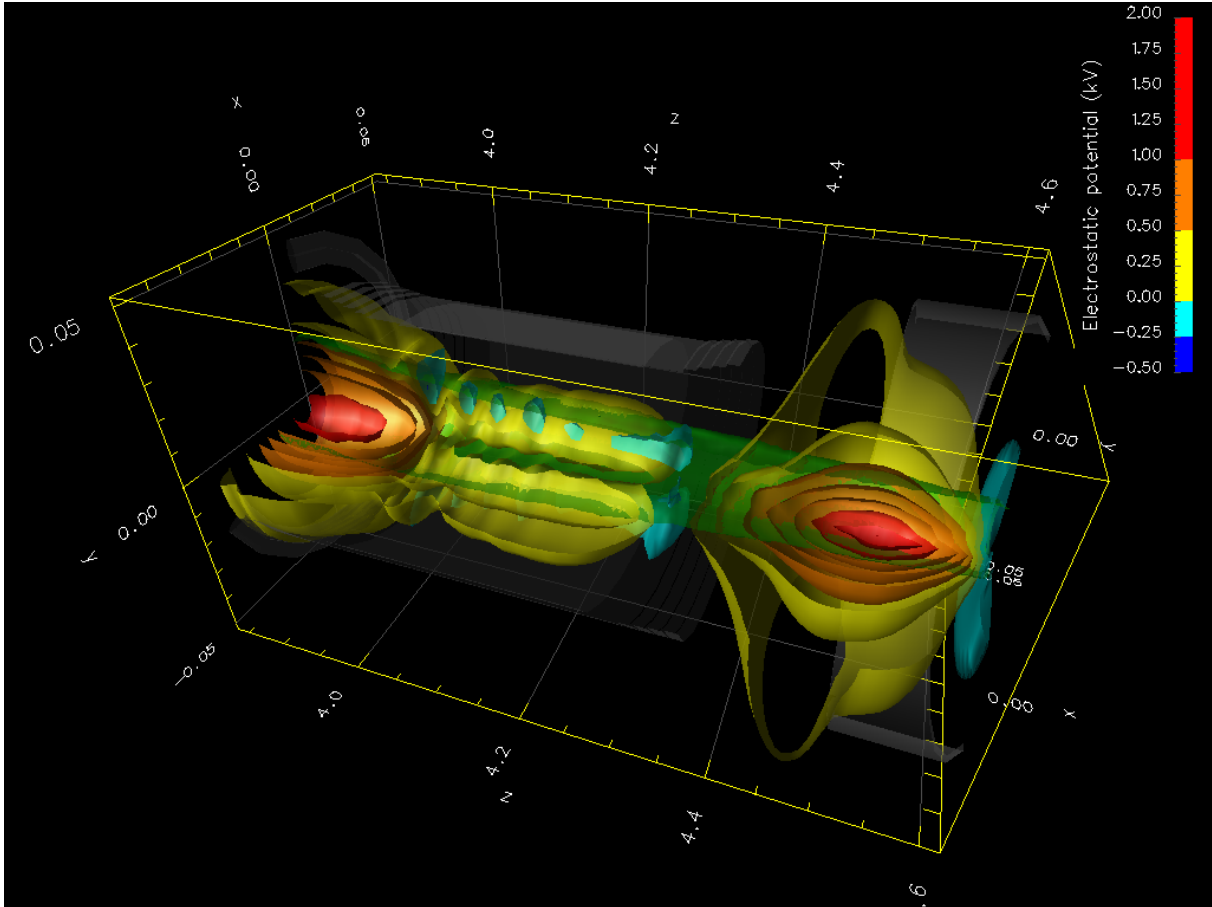
FIG. 7: Snapshot of equipotential surfaces from WARP-POSINST simulation of HCX at $t = 3\ \mu$s.

search.

[1] Proc. 31st ICFA Advanced Beam Dynamics Workshop on Electron-Cloud Effects (ECLOUD'04), Napa, CA, USA, 19-23 Apr 2004, CERN Report CERN-2005-001 (2005), ISBN 92-9083-241-X, http://icfa-ecloud04.web.cern.ch/icfa-ecloud04/agenda.html

[2] L. R. Prost, P. A. Seidl, F. M. Bieniosek, C. M. Celata, A. Faltens, D. Baca, E. Henestroza, J. W. Kwan, M. Leitner, W. L. Waldron, R. Co-
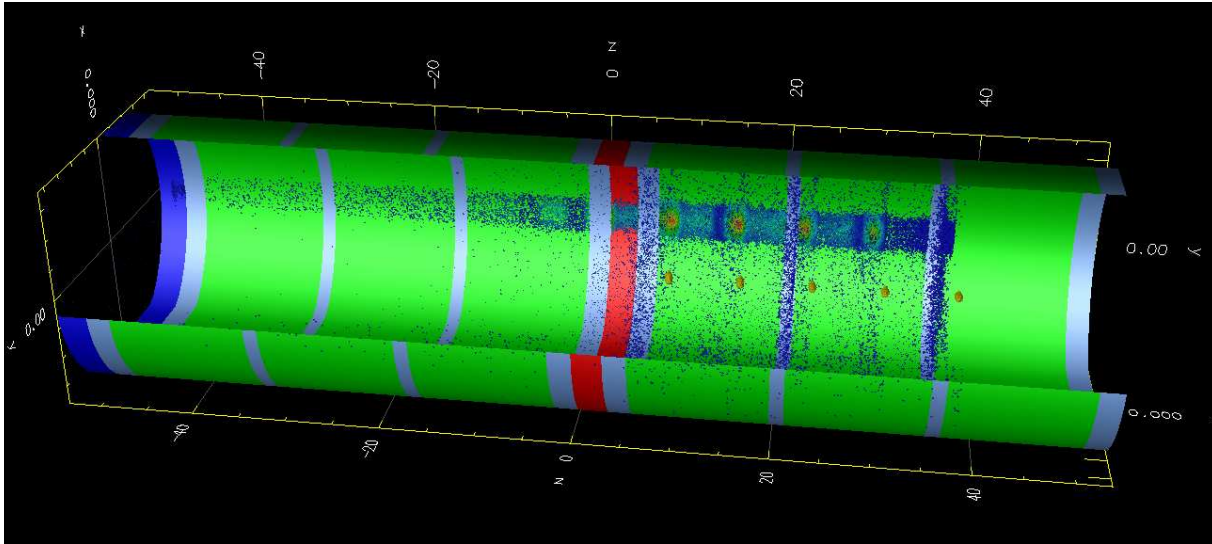
FIG. 8: Snapshot from a 3-D self-consistent simulation of five bunches (yellow) propagating (from left to right) in one LHC arc FODO cell (green: dipoles; blue: focusing quad; red: defocusing quad; silver: drift) and interacting with electrons. The electrons are generated by photo-emission (80% direct synchrotron emission from the bunches plus 20% background radiation) and secondary emission, and are colored according to electron density (rainbow palette; low: blue; high: red).

hen, A. Friedman, D. Grote, S. M. Lund, A. W. Molvik, and E. Morse, *PRST-AB* **8**, 020101 (2005).

[3] *The Large Hadron Collider: Conceptual Design*, CERN/AC/95-05 (LHC), Oct. 1995, Chapter 2, Figs. 1 and 2.

[4] D. P. Grote, A. Friedman, J.-L. Vay. I. Haber, *AIP Conf. Proc.* **749**, 55 (2005)

[5] M. A. Furman and G. R. Lambertson, Proc. Intl. Workshop on Multibunch Instabilities in Future Electron and Positron Accelerators "MBI-97," KEK, p. 170; M. A. Furman, LBNL-41482/LHC Project Report 180, May 20, 1998.

[6] M. A. Furman and M. T. F. Pivi, PRSTAB/v5/i12/e124404 (2003).

[7] Vay, J-L.; Furman, M.; Cohen, R.; Friedman, A.; Grote, D., Proc. 21st Biennial Particle Accelerator Conference, PAC05, Knoxville, TN, (2005)

[8] http://www.txcorp.com/technologies/TxPhysics

[9] J.-L. Vay, et al, *Phys. of Plasmas* **11**, 2928 (2004).

[10] J.-C. Adam, A. Gourdin Serveniere, A. B. Langdon, *Journal of Comput. Physics* **47**, 229-244 (1982)

[11] R. H. Cohen, A. Friedman, D. P. Grote, J.-L. Vay, These Proceedings

[12] R. H. Cohen, et al, *Phys. of Plasmas* **12** (2005)

[13] A. W. Molvik, et al, *PRST-AB* **7**, 093202 (2004).

[14] http://srim.org

[15] P. H. Stoltz, M. A. Furman, J. L. Vay, A. W. Molvik and R. H. Cohen, *PRSTAB* **6**, 054701 (2003).

[16] C. K. Birdall, *IEEE Transactions on plasma science* **19**, 2 (1991)

[17] A.W. Molvik, et al, Proc. 21st Biennial Particle Accelerator Conference, PAC05, Knoxville, TN, (2005)

[18] J.-L. Vay, M. A. Furman, R. H. Cohen, A. Friedman, D. P. Grote, Proc. 21st Biennial Particle Accelerator Conference, PAC05, Knoxville, TN, (2005)

[19] Benedetto et. al., *PRST-AB* **8**, 124402 (2005)

[20] http://wwwslap.cern.ch/collective/electron-cloud/Programs/Headtail/headtail.html

[21] G. Rumolo et. al., *PRST-AB* **6**, 081002 (2003).